



## Journal of Pharmaceutical Research

## ORIGINAL ARTICLE

## Formulation and Evaluation of Solid Lipid Nanoparticles of Etravirine

M S Roopa<sup>1</sup>, Arti Mohan<sup>1,\*</sup><sup>1</sup>Department of Pharmacy, Krupanidhi College of Pharmacy, Carmelaram, Varthur Hobli, Bengaluru, Karnataka, India

## ARTICLE INFO

## Article history:

Received 12.09.2018

Accepted 18.11.2018

Published 22.12.2018

## \* Corresponding author.

Arti Mohan

[artimohan89@gmail.com](mailto:artimohan89@gmail.com)[https://doi.org/](https://doi.org/10.18579/jopcr/v17.4.roopa)[10.18579/jopcr/v17.4.roopa](https://doi.org/10.18579/jopcr/v17.4.roopa)

## ABSTRACT

**Objectives:** Solid lipid nanoparticles (SLNs) are submicron colloidal carriers with an average diameter of nanometers. Owing to their inherent biodegradability and biocompatibility, lipids are now being extensively investigated as carriers for drugs and proteins. The aim of the present study was to formulate and evaluate SLNs containing etravirine, considering the assessment of its poor solubility and low bioavailability from the conventional dosage form.

**Methods:** The formulations were prepared by high-pressure homogenization technique using different lipid-surfactant ratios, while keeping the quantities of the active ingredient constant. Nine different formulations were prepared. The nanoparticles obtained were characterized for particle size analysis, zeta potential analysis, scanning electron microscopy (SEM), differential scanning calorimetry (DSC), Fourier-transform infrared spectroscopy (FTIR), drug content and in vitro drug release profile, stability, and comparative dissolution study of the pure drug and optimized formulation.

**Findings:** Etravirine solid lipid nanoparticle formulations were characterized, and the particle size and surface charge were found to be 234.26 nm and -42.4 mV. The drug loading capacity of the particle was found to be 29.90%, and the in vitro release study of optimized formulations in phosphate buffer pH 6.8 with 1% sodium lauryl sulphate exerted a precise release of 96.48% over a period of 90 min. SEM analysis of the optimized formulation revealed that the particles were slightly spherical.

**Novelty:** Formulation of solid lipid nanoparticles can be easily prepared with adequate physical properties and the required particle size and release characteristics which might be an advantage for oral administration.

**Keywords:** Etravirine; solid lipid nanoparticles; particle size; zeta potential; entrapment efficiency; drug release

## INTRODUCTION

Nanotechnology offers many advantages such as targeted drug delivery and controlled/programmed release of therapeutic compounds for improved drug pharmacokinetics, biodistribution, and pharmacodynamic activity. In addition, this strategy can be implemented for drugs belonging to Biopharmaceutics Classification System (BCS) class II and IV to increase their solubility and permeation through the gastrointestinal (GI) barrier. It can be used to solve problems associated with poorly soluble drugs, thereby increasing their solubility and bioavailability<sup>1,2</sup>. In recent years, lipid-based nanoparticles have gained attention for drug delivery owing to their physiochemical diversity, biocompatibility, and ability to enhance the oral bioavailability of poorly water-soluble drugs<sup>3,4</sup>. Matrix-type lipid-based Solid Lipid

Nanoparticles (SLNs) represent an alternative carrier system to conventional colloidal systems such as emulsions, liposomes, and polymeric micro- and nanoparticles. SLN are submicron colloidal carriers with particle sizes ranging from 50-1000 nm. SLN are biocompatible and biodegradable and have been used for controlled drug delivery and specific targeting. It also offers greater surface area, prolonged drug release, and instant uptake by cells. The potential of this approach lies in its ability to address the issues of poor solubility and low bioavailability of drugs. Increasing the rate of dissolution and tissue distribution can improve the bioavailability of poorly soluble drugs and entrapped drugs. This approach holds great promise in overcoming the limitations of traditional drug delivery methods<sup>5,6</sup>. It can be administered via various routes and can incorporate

hydrophilic/hydrophobic drugs with different physicochemical and pharmacological properties<sup>7,8</sup>.

Antiretroviral (ARV) drugs are clinically accepted for the effective management of Acquired Immune Deficiency Syndrome (AIDS) by controlling Human Immunodeficiency Virus (HIV). Etravirine (ETR) is a non-nucleoside reverse transcriptase inhibitor (NNRTI) that was developed for the treatment of HIV-1 infection. It is a BCS class IV compound with a low solubility and permeability. At LogP values greater than 5, the substance is practically insoluble across a broad range of physiological pH levels and is metabolized by cytochrome P450<sup>9,10</sup>.

New approaches to drug delivery have emerged in order to attain the objectives of ARV therapy in the context of HIV/AIDS management<sup>11</sup>. SLNs have been investigated as potential antiviral agents that target the lymphatic system<sup>12</sup> to enhance oral bioavailability. It addresses solubility problems and minimize drug toxicity and extensive first-pass metabolism. Therefore, SLNs have a significant potential for delivering drugs to specific sites within the body in a controlled manner. To ensure safety, the lipids utilized in the preparation of SLNs should be biocompatible and should remain solid at body temperature. Since not much work has been reported on ETR-SLN preparation, in this study, ETR-SLN was prepared and evaluated these SLNs of Etravirine for its solubility and bioavailability from the conventional dosage form.

## METHODS

### *Pre-formulation studies*

Preformulation testing provides useful data for formulators to develop stable and bioavailable dosage forms.

### *Melting point determination*

The Thiel's tube method for melting point determination was used in the present study.

### *FTIR Spectrum of Etravirine*

Fourier-transform infrared spectroscopy (FTIR) was used to identify the major peak positions of etravirine. The sample was analyzed using the potassium bromide pellet method in an IR spectrophotometer (Bruker) in the region between 4000-400  $\text{cm}^{-1}$ <sup>13</sup>.

### *Solubility Studies of Etravirine in lipids*

The lipids (200 mg) were weighed and melted. A saturated solution of the drug in melted lipid was prepared. Drug lipids (100 mg) were dissolved in methanol, centrifuged for 2 h, and a saturated clear solution was taken and diluted to Beer's range of concentrations. The absorbance of these solutions was measured against methanol as a blank using UV spectroscopy<sup>14</sup>.

### *UV spectrophotometric method for estimation of etravirine - Determination of lambda max of Etravirine*

A stock solution of 1 mg/ml etravirine was prepared by dissolving 100 mg of the drug in 100 ml of phosphate buffer solution (PBS) at pH 6.8 +1% sodium lauryl sulphate (SLStock I (S) (1000  $\mu\text{g}/\text{mL}$  stock I). Stock I (5 ml of stock I was further diluted to 50 ml using PBS pH 6.8+1% SLS (100  $\mu\text{g}/\text{ml}$  - Stock II). From stock II, aliquots were prepared and diluted to 10 ml using phosphate buffer (pH 6.8+1% SLS) in a volumetric flask to obtain a concentration of 5-35  $\mu\text{g}/\text{ml}$ . The resultant solution was scanned for  $\lambda$  max between 200-400 nm and etravirine showed maximum absorbance at 310 nm<sup>15,16</sup>.

### *Calibration curve of Etravirine in Phosphate buffer solution (PBS pH 6.8+1% SLS)*

A stock solution of 1 mg/ml of Etravirine was prepared by dissolving 100 mg of drug in 100 ml of Phosphate buffer solution (PBS) pH 6.8+1% SLS (1000  $\mu\text{g}/\text{ml}$  - stock I). 5 ml of stock I was further diluted to 50 ml using PBS pH 6.8+1% SLS (100  $\mu\text{g}/\text{ml}$  - Stock II). From stock II, 0.5 ml, 1 ml, 1.5 ml, 2 ml, 2.5 ml and 3 ml were taken and volume was diluted to 10 ml using Phosphate buffer pH 6.8+1% SLS. The dilutions were scanned for maximum absorbance in a UV-visible double beam spectrophotometer in the range of 400 to 800 nm using phosphate buffer pH 6.8+1% SLS as a blank<sup>15,16</sup>.

### *The Linear Regression Analysis*

Linear regression analysis was performed on the absorption points to obtain the regression equations, correlation coefficients, slopes, and intercepts.

### *Compatibility studies*

A compatibility study was performed using Fourier-transform infrared spectroscopy. The compatibility between the drug, lipid, and surfactant, as well as the optimized formulation, was determined by FTIR using a Shimadzu FT-IR spectrophotometer. The potassium bromide (KBr) pellet method was used in this study. The samples were thoroughly blended with dry potassium bromide crystals. The mixture was then compressed to form a disc. The disc was placed in the sample cell and the spectrum was recorded between 400-4000  $\text{cm}^{-1}$ . The FTIR spectra of the pure drug, the drug with excipients, and the optimized formulation were recorded and compared.

### *Formulation and design of Solid lipid nanoparticles (SLNs)*

#### *Formulation design*

Custom design was inculcated to obtain different experimental runs using design JMP software version 13, which analyzes the main effects and certain interactions and also

helps to identify the significant factors from those which are not significant. The independent variables were glyceryl monostearate and poloxamer 188 percentage concentration, stirring speed, stirring time, and cooling temperature. The lower and higher levels of independent factors were selected based on the literature and initial screening experiments. The factors and their levels are listed in Table 1.

Table 1: Composition

Formulation Code	Gms (%)	Poloxamer (%)	Stirring Speed (Rpm)	Stirring Time (Min)	Cooling
F1	2	1	15000	15	High
F2	5	1	15000	15	Low
F3	5	1	30000	15	High
F4	5	3	30000	30	Low
F5	2	1	15000	30	Low
F6	5	3	15000	30	High
F7	2	3	30000	15	Low
F8	3.5	2	22500	22.5	High
F9	2	3	30000	30	High

#### Method of preparation of solid lipid nanoparticles

The lipid (glyceryl monostearate) melted above its melting point. The drug was dissolved in melted lipid and stirred using a magnetic stirrer to form a pre-emulsion. The emulsion was dispersed in the surfactant in poloxamer 188 and subjected to homogenization at 25,500 rpm for 22.5 min which led to the formation of hot oil in water. The SLNs were then cooled to room temperature<sup>17</sup>.

#### Evaluation of solid lipid nanoparticles

##### Physical evaluation and percentage yield determination

The percentage yield of solid lipid nanoparticles for all formulations was calculated by considering the final weight of the product after drying in comparison to the total weight of the drug, polymer, and other excipients, such as glyceryl monostearate, used for the preparation of solid lipid nanoparticles. The percentage yield of the product was calculated using the following equation:

$$W0\% \text{ Practical yield} = \frac{\text{_____}}{\text{_____}} \times 100 \text{ WT}$$

Where, W0 - Practical mass of Etravirine SLNs WT - Theoretical mass

##### Determination of Drug content, loading and entrapment efficiency drug content

A formulation equivalent to 250 mg of drug was dissolved in a small quantity of phosphate buffer pH 6.8 containing 1% SLS. The solution was made up to 250 ml using a phosphate buffer pH 6.8 containing 1% SLS. One millilitre of this

solution was diluted to 10 ml with phosphate buffer pH 6.8 containing 1% SLS. The absorbance of this solution was measured at 310 nm<sup>18</sup>.

##### Determination of loading and entrapment efficiency

The etravirine content in the nanoparticles was estimated using UV-visible spectrophotometry. Formulations equivalent to 10 mg of particles from each batch were dissolved in 10 ml of phosphate buffer pH 6.8 containing 1% SLS under vigorous vortexing. The solution was centrifuged, and the supernatant was further diluted with buffer to ensure that the absorbance was within the linearity range. The analysis was performed in triplicate for each batch<sup>14,19</sup>.

##### Determination of Particle size and Zeta potential:

##### Determination of Particle size (Malvern particle size analyzer/ Zetasizer)

It can be analyzed using a Malvern particle size analyzer. The larger the particle, the slower the motion, and hence the smaller the variation in the intensity of scattered light. Photon-correlation spectroscopy uses the rate of change in intensity to determine the size distribution of the particles. The Zetasizer has a correlator with 64 channels. Each channel measures changes in light fluctuation over a defined time span. The time span is known as the sample time or delay time, and the correlator measures the light intensity by counting the photons. For a very short time period, the changes in light intensity will be very small because the particles have very little time to move, and the position of the particles can be statistically defined as being highly correlated. In contrast, with a long sample time, particles will move randomly from their initial positions, and the particles can be statistically described as not being correlated<sup>20</sup>.

##### Determination of Zeta potential (Malvern Zetasizer)

The zeta potential of SLNs was measured using a Malvern Zetasizer. The Zetasizer consists mainly of a laser used to provide a light source to illuminate the particles within the sample. For zeta potential measurements, this light split provides incident and reference beams. The incident laser beam passed through the centre of the sample cell and scattered light at an angle of approximately 13° was detected. When an electric field is applied to the cell, any particle moving through the measurement volume causes the intensity of light to fluctuate with a frequency proportional to the particle speed, which is passed to the digital signal processor and then to a computer. The Zetasizer software produces a frequency spectrum from which electrophoretic mobility takes place; hence, the zeta potential is calculated<sup>21</sup>.

##### In vitro dissolution studies

In vitro drug release from etravirine was determined using a type II apparatus (paddle type). A weighed amount of

etravirine solid lipid nanoparticles equivalent to 200 mg of drug was placed in a dissolution chamber containing 900 ml of phosphate buffer pH 6.8 containing 1% SLS. The temperature of the dissolution chamber was maintained at  $37^{\circ}\text{C} \pm 0.5^{\circ}\text{C}$  with a rotation speed of 100 rpm. Samples (1 ml) were withdrawn at predetermined time intervals of 5, 10, 15, 30, 45, 60, and 90 min, and the same volume of release medium was added to maintain the sink conditions. The sample at each time interval was diluted and analysed spectrophotometrically at 310 nm to determine the amount of etravirine in the sample, the absorbance was noted, and the % CDR was calculated<sup>22</sup>.

### **Optimization studies**

Commercially available JMP software, version-13 was used to study the effect of the concentration of lipids, surfactants, stirring speed, stirring time, and cooling factors on the particle size of solid lipid nanoparticles of etravirine. Analysis was performed using ANOVA at a significance level of  $P < 0.05$ . optimization was achieved with a desirability of 0.5249. v. The optimized formula consisted of glyceryl monostearate 3.5%, Poloxamer-188 (2%), stirring speed (22500 rpm), and stirring time (22.5 min) with low cooling.

### **Physical evaluation and % yield of optimized formula**

Physical evaluation and percentage yield of the optimized formulation were determined.

### **Determination of drug content, drug loading and entrapment efficiency**

The drug content, drug loading, and entrapment efficiency of the optimized formulations were determined.

### **Cumulative drug release of pure drug and optimized formulation**

The cumulative drug release of the pure drug and the optimized formulation was determined.

### **Determination of particle size and zeta potential**

Particle size, polydispersity index, and zeta potential of the optimized formulations were determined.

### **Differential scanning calorimetry (Mettler- Toledo DSC 1**

Both the sample and the reference were maintained at the same temperature throughout the experiment. Generally, the temperature program for differential scanning calorimetry (DSC) analysis is designed such that the sample holder temperature increases linearly with time. Differential scanning calorimetry was used to measure the amount of heat absorbed or released during such transitions by observing the difference in heat flow between the sample and the reference<sup>23</sup>.

### **Scanning electron microscopy (SEM)**

The surface morphology of the specimens was determined using a scanning electron microscope. A scanning electron microscope (SEM) is a type of electron microscope that produces images which result from interactions of the electron beam with atoms at various depths within the sample. The electrons interact with atoms in the sample, producing various signals that contain information regarding the surface topography and composition of the sample<sup>24</sup>.

### **Stability studies**

The optimized formulation was subjected to accelerated stability studies in a stability chamber for 30 days at  $40 \pm 2^{\circ}\text{C}$  and  $75 \pm 5\%$  RH. The formulation was evaluated for appearance, drug content, and in vitro drug release after 30 days.

## **RESULTS AND DISCUSSION**

A literature review was carried out to determine the QTPP, CQAs, and manufacturing procedures for SLN, as well as the various processes and formulation attributes that impact product CQAs. The intended solid lipid nanoparticulate drug delivery system has been reported to be used for various routes of administration, including oral, parenteral, dermal, ocular, nasal, etc., for topical, systemic, or central nervous system actions. To achieve optimal drug absorption, it is essential to use small nanoparticles. Therefore, the minimum average particle size is one of the CQAs, along with the minimum PDI (monodispersity), maximum entrapment efficiency, minimum zeta potential of  $\pm 20$  mV for stability<sup>25</sup>, and absence of any residual solvent to ensure safety and avoid toxicity. CQA refers to a physical, chemical, biological, or microbiological attribute that must fall within a specific limit, range, or distribution to guarantee the desired level of product quality<sup>26,27</sup>. During this study, various preliminary trials were conducted to identify suitable excipients or materials that could directly or indirectly affect critical quality attributes.

Improved permeability of the drug has been reported because of the lipid content in SLN<sup>28</sup>. SLN contain lipids which remain solid at room and body temperatures. Lipids include pure triglycerides (tristearin, tripalmitin, trimyristin, etc.), long-chain alcohols (acetyl alcohol), waxes (bees wax, acetyl palmitate), and sterols (cholesterol)<sup>29</sup>.

### **Pre-formulation studies**

#### **Melting point determination**

The melting point of etravirine was found to be  $264^{\circ}\text{C}$ .

#### **FTIR Spectrum of Etravirine**

A small amount of the drug sample was studied for its functional characteristics using FTIR spectroscopy, and the peaks obtained were analyzed for their functional groups



(Table 2).

### Solubility studies of Etravirine in lipids

Solubility studies were performed using lipids (glyceryl behenate, glyceryl monostearate, and stearic acid), and the saturation solubility of the drug in lipids was determined. From the result, glyceryl monostearate showed more solubility of about 13.10 mg/ 200 mg, followed by stearic acid (12.00 mg / 200 mg) and glyceryl behenate (8.6 mg / 200 mg).

### UV spectrophotometric method for estimation of etravirine

#### Determination of lambda max of Etravirine

The  $\lambda_{max}$  of etravirine was 310 nm at a concentration of 35  $\mu$ g/ml and the absorbance was 0.772 (Figure 1).

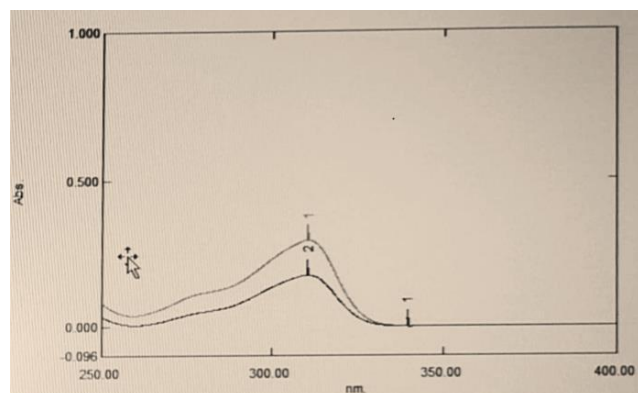


Fig. 1: UV scan of Etravirine with Phosphate buffer 6.8 +1%SLS

### Calibration curve of Etravirine

The calibration curve was plotted at concentrations of 5, 10, 15, 20, 25, 30, and 35  $\mu$ g/ml etravirine. In pre-formulation studies, it was found that the estimation of Etravirine by UV spectrophotometry at 310 nm had good reproducibility. The regression coefficient was 0.9986 and the slope was 0.0218.

### Compatibility studies

The aim of the drug excipient compatibility study was to determine the potential interactions between the drug and excipients in the formulation using FTIR. The comparison of the optimized formulation's spectra with those of etravirine (the pure drug) and the physical mixture can be observed in Table 2. According to FTIR analysis, there was no apparent interaction between the functional groups in the formulation, as no such frequencies were observed. Hence, the peak stretching remains unchanged, which indicates that the drug and lipid are compatible.

Table 2: FTIR spectrum data of Etravirine, drug and excipients

FTIR Spec-trum	Functional group	Stretching peak range (cm <sup>-1</sup> )	Observed Peak range (cm <sup>-1</sup> )
Etravirine	C-H stretching aliphatic	3000-2840	2918.1
	N-H aromatic primary amines	3500-3300	3349.2
	C≡N nitrile	2250-2200	2223.5
	C-N stretching aliphatic amines	1250-1020	1243.7
	C-O-C ether stretching	1300-1000	1199.4
	N-H stretching primary, secondary amines	910-665	713.3
FTIR Spec-trum	Functional group	Stretching peak range (cm-1)	Observed Peak range (cm-1)
Etravirine	C-H stretching aliphatic	3000-2840	2918.1
	N-H aromatic primary amines	3500-3300	3349.2
	C≡N nitrile	2250-2200	2223.5
	C-N stretching aliphatic amines	1250-1020	1243.7
	C-O-C ether stretching	1300-1000	1199.4
	N-H stretching primary, secondary amines	910-665	713.3
Etravirine + Glyceryl monos-tearate + Polox-amer	C-H stretching aliphatic	3000-2840	2916.9
	N-H amines	3500-3300	3380.8
	C≡N nitrile	2250-2200	2223.6
	C-N stretching aliphatic amines	1250-1020	1243.2
	C-O-C ether stretching	1300-1000	1199.4
	N-H stretching primary, secondary amines	910-665	718.2
Optimized formu-lation	C-H stretching aliphatic	3000-2840	2916.5
	N-H amines	3500-3300	3348.9
	C≡N nitrile	2250-2200	2223.2
	C-N stretching aliphatic amines	1250-1020	1243.1
	C-O-C ether stretching	1300-1000	1199.0
	N-H stretching primary, secondary amines	910-665	718.3

### **Formulation and design of SLNs**

Nine formulations of etravirine lipid nanoparticles were devised using a custom design. Solid lipid nanoparticles were formulated using a hot homogenization method. The preparation of nanoparticles involved maintaining a constant concentration of the drug while varying the lipid ratio and surfactant concentration. Nine different formulations were prepared.

### **Evaluation of solid lipid nanoparticles**

#### **Physical evaluation and percentage yield determination**

The percentage yield of the prepared formulations ranged from 82.50% to 97.89%. The percentage drug content of the prepared formulations was noted between 82.70%–94.64%. The percentage yield and percentage of drug content are shown in Table 3.

#### **Determination of Drug content, loading and entrapment efficiency**

The entrapment efficiency and drug loading of all the formulations range from 47.77% to 85.71% and 12.21% to 28.95%, respectively (Table 3).

#### **UV spectrophotometric method for estimation of etravirine - Determination of particle size and zeta potential**

The attainable particle size is influenced by the composition and concentration of lipids and emulsifiers<sup>30</sup>. Particles with a size of 200 nm were produced using polyhydroxy surfactants<sup>29</sup>, while nanoparticles ranging from 180 to 190 nm were created with acetyl palmitate as a lipid, which has been reported to be effective for targeting the brain<sup>28</sup>, and sizes of up to 140 nm were achieved for acetyl palmitate SLN when the lipid nanoparticle formulation was optimized using a computer-generated experimental design. In general, an average size of 20–500 nm is reported depending on the drug, lipid, surfactants, and formulation technique used<sup>31</sup>. The particle size analysis data of formulations F1 to F9 obtained by the Malvern Zetasizer indicate the average particle size and polydispersity index which were observed between 134.4 nm to 1127 nm and 0.247–0.856, respectively. A polydispersity index less than 1 indicates that the particle size distribution is uniform. The particles were within the acceptable nanometer range. Zeta potential analysis was conducted to obtain information on the surface properties of nanoparticles. As a rule of thumb, a zeta potential above  $\pm 30$  mV is considered physically stable. The zeta potential of F1 to F9 formulations was observed between -20.3 mV to -34.4 mV (Table ??). The zeta potential is a crucial physicochemical parameter that affects the stability of nanosuspensions. Highly positive or negative zeta potential values result in stronger repulsive forces, whereas the

repulsion between particles with similar electric charges prevents aggregate formation and facilitates easy redispersion. For nanosuspensions stabilized by both electrostatic and steric forces using large molecular weight stabilizers, a zeta potential of  $\pm 20$  mV is typically desirable<sup>25</sup>.

### **In vitro dissolution studies**

In vitro drug release data from the solid lipid nanoparticles were obtained for 90 min and graphically represented as % CDR vs. time profile. Of the nine formulations, F8 showed a good drug release of 96.46%. Drug release profiles are shown in Table ???. These findings suggested that drug release from the SLN dispersion was more consistent than that from the plain drug suspension. The initial burst release was followed by sustained release, in agreement with other studies<sup>32</sup>. The developed formulation included surfactants and featured small-sized nanoparticles, which likely enhanced the drug's permeability, wetting, solubilization, and dissolution. Additionally, these factors may have contributed to the formation of pores in the matrix, leading to a consistent and improved drug release. Similar outcomes were also observed, and it was noted that nanosized drug delivery systems can improve the delivery of drugs to the brain through the nose compared to formulations in equivalent drug solutions. The reason behind this effect could be attributed to the preservation of the drug from breakdown and/or its re-entry into the nasal passage<sup>33</sup>.

### **Optimization - Evaluation of optimized formulation**

The experimental (actual) and predicted values of optimized Etravirine solid lipid nanoparticle formulations were compared and were discovered to be in close agreement with one another, indicating the appropriateness of the optimization process in the successful development of the etravirine SLN formulation.

#### **Physical evaluation and % yield of optimized formulation**

The optimized formulation was observed to be an off-white powder with a yield of 95.25%.

#### **Determination of Drug content, drug loading and entrapment efficiency**

The drug content of the optimized formulation  $\pm$  SD (n=3) was 95.21% and the drug loading was 29.90%. The entrapment efficiency was 85.82%.

#### **Cumulative drug release of Pure drug and optimized formulation**

The optimized formulation of etravirine lipid nanoparticles demonstrated a higher drug release rate of 96.48%, in contrast to the pure drug etravirine, which showed a release rate of 37.46%. This information is presented in Table ??.

**Table 3: Physical evaluation, Drug content, Entrapment efficiency and Drug loading**

Sr. No	Formulation code	Appearance	Percentage Yield (%)	Drug content (%)	Drug loading (%)	Entrapment Efficiency (%)
1	F1	Off white powder	90.75	92.85 $\pm$ 0.03	22.21 $\pm$ 0.63	61.07 $\pm$ 1.98
2	F2	Off white powder	96.53	91.96 $\pm$ 0.026	12.21 $\pm$ 0.98	71.82 $\pm$ 2.31
3	F3	Off white powder	84.98	89.20 $\pm$ 0.032	20.36 $\pm$ 1.26	53.58 $\pm$ 0.92
4	F4	Off white powder	96.27	90.17 $\pm$ 0.029	13.12 $\pm$ 2.36	78.13 $\pm$ 1.87
5	F5	Off white powder	82.50	82.70 $\pm$ 0.016	19.45 $\pm$ 1.84	72.39 $\pm$ 2.23
6	F6	Off white powder	95.89	91.07 $\pm$ 0.032	12.66 $\pm$ 1.34	75.41 $\pm$ 1.56
7	F7	Off white powder	94.66	87.50 $\pm$ 0.012	16.28 $\pm$ 0.78	47.77 $\pm$ 3.25
8	F8	Off white powder	97.86	94.64 $\pm$ 0.021	28.95 $\pm$ 0.81	85.71 $\pm$ 2.53
9	F9	Off white powder	97.08	93.75 $\pm$ 0.039	27.60 $\pm$ 0.57	82.88 $\pm$ 1.76

### Determination particle size and Zeta potential of optimized formulation

The particle size analysis data of the optimized formulations obtained by the Malvern Zetasizer indicated an average particle size of 234.26 nm with a polydispersity index of 0.294. A polydispersity index less than 1 indicates that the particle size distribution is uniform. The particles were within the acceptable nanometer range. Zeta potential analysis was performed to obtain information on the surface properties of nanoparticles. As a rule of thumb, a zeta potential above  $\pm 30$  mV is considered physically stable. The zeta potential of the optimized formulations was -42.4 mV showing excellent stability.

### Differential scanning calorimetry

The thermal behaviour of etravirine and the optimized SLNs formulations was investigated using differential scanning calorimetry (DSC) to observe the effect of lipids on etravirine. The DSC thermogram of etravirine showed an endothermic peak at 264.83°C with an onset at 260.01°C and an end set at 265.58°C that corresponds to the melting point of etravirine. It was noticed that there was a shift in the melting point from 264.83°C to 255.13°C which indicates that Etravirine must be molecularly dispersed in the formulations (Figure 2).

### Scanning electron microscopy

Scanning electron microscopy (SEM) was performed to optimize the formulation. It was observed that the particles were discrete, without significant clumping. The surfaces appeared uneven, and the particles were slightly spherical,

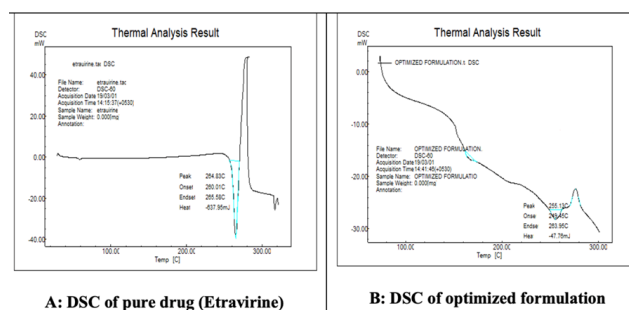


**Fig. 2: a: DSC of pure drug (Etravirine); b: Optimized formulation**

as shown in Figure 3.

### Stability studies

The optimized formulation was subjected to short-term stability studies for 30 days at 40°C  $\pm$  2°C / 75%  $\pm$  5% RH. Physical and chemical changes were observed throughout the study period. Physical stability was analyzed by morphological appearance, and chemical stability was analyzed by changes in the release profile. The results revealed no significant changes in the morphological appearance or release profile. The formulations were stable at 40 $\pm$ 2°C and 75 $\pm$ 5% RH.

### CONCLUSION

In the current study, etravirine solid lipid nanoparticles were successfully developed using a combination of glyceryl

**Table 4: Particle size, Polydispersity index and Zeta potential, Cumulative drug release studies (F1-F9) and In vitro drug release profile of Pure drug and optimized formulation**

Formulation Code	Particle size (nm)	Log Particle size	Polydispersity index (PDI)	Zeta potential (mV)
F1	1127	3.051924	0.856	-31.5
F2	800	2.90309	0.684	-20.2
F3	174.1	2.240799	0.312	-30.2
F4	271.9	2.434409	0.531	-20.3
F5	555	2.744293	0.588	-27.3
F6	600	2.778151	0.630	-20.5
F7	499	2.434409	0.684	-34.4
F8	271.9	2.698101	0.510	-29.5
F9	134.4	2.128399	0.247	-31.6

**Time % Cumulative drug release**

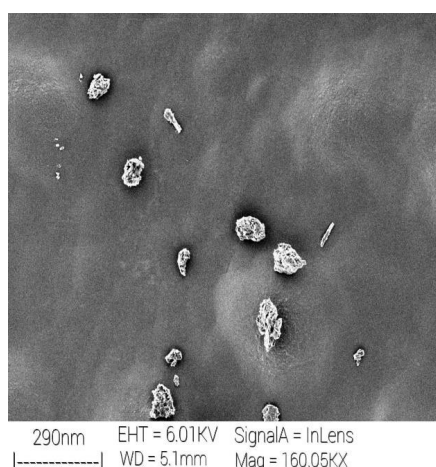
(min)

	F1	F2	F3	F4	F5	F6	F7	F8	F9
0	0	0	0	0	0	0	0	0	0
5	9.70	10.64	15.45	13.5	12.78	11.58	15.56	22.39	21.84
10	20.29	22.17	28.18	23.4	27.54	24.95	22.38	35.41	35.83
15	34.41	27.49	36.36	36.00	38.36	31.88	35.03	48.94	45.44
30	44.15	42.56	47.27	51.31	45.24	43.13	47.68	58.57	58.95
45	63.53	50.55	66.37	63.02	58.03	52.45	65.19	69.76	63.79
60	75.22	65.62	75.46	80.11	71.80	64.16	80.76	85.27	76.9
90	81.18	77.46	86.37	92.71	84.59	79.3	92.44	96.46	94.38

**Time % Cumulative drug release  $\pm$  SD (n=3)**

(min)

	Pure drug	OF1
0	0	0
5	10.58 $\pm$ 0.267	25.97 $\pm$ 0.231
10	17.10 $\pm$ 0.492	38.03 $\pm$ 0.324
15	23.61 $\pm$ 0.263	49.17 $\pm$ 0.142
30	27.69 $\pm$ 0.396	64.94 $\pm$ 0.423
45	30.95 $\pm$ 0.364	77.00 $\pm$ 0.361
60	33.39 $\pm$ 0.296	89.06 $\pm$ 0.263
90	37.46 $\pm$ 0.216	96.48 $\pm$ 0.293

**Fig. 3: Scanning electron microscopy of optimized formulation**

monostearate and poloxamer-188 through a high-pressure homogenization method to improve the drug dissolution rate. This method was simple, reproducible, and capable of producing solid lipid nanoparticles without the use of organic solvents, making it feasible for large-scale production. Additionally, the lipid nanoparticles created in this study serve as effective carrier systems for incorporating various bioactive compounds for oral administration. This research demonstrated the successful enhancement of the



drug dissolution rate with the formulated etravirine solid lipid nanoparticles.

## REFERENCES

1. Suri SS, Fenniri H, Singh B. Nanotechnology-based Drug Delivery Systems. *Current Research in Pharmaceutical Technology*. 2011;2:1–8. Available from: <https://ocup-med.biomedcentral.com/articles/10.1186/1745-6673-2-16>.
2. Dizaj SM, Vazifehasl Z, Salatin S, Adibkia K, Javazadeh Y. Nanosizing of drugs: effect on dissolution rate. *Research in pharmaceutical sciences*. 2015;10:95–108. Available from: [https://www.researchgate.net/publication/281873785\\_Nanosizing\\_of\\_drugs\\_Effect\\_on\\_dissolution\\_rate#:~:text=According%20to%20the%20reviewed%20literature,dissolution%20rate%20would%20be%20enhanced](https://www.researchgate.net/publication/281873785_Nanosizing_of_drugs_Effect_on_dissolution_rate#:~:text=According%20to%20the%20reviewed%20literature,dissolution%20rate%20would%20be%20enhanced).
3. Kalepu S, Manthina M, Padavala V. Oral lipid-based drug delivery systems – an overview. *Acta Pharmaceutica Sinica B*. 2013;3(6):361–372. Available from: <https://dx.doi.org/10.1016/j.apsb.2013.10.001>.
4. Das S, Chaudhury A. Recent Advances in Lipid Nanoparticle Formulations with Solid Matrix for Oral Drug Delivery. *AAPS PharmSciTech*. 2011;12(1):62–76. Available from: <https://dx.doi.org/10.1208/s12249-010-9563-0>.
5. Müller RH, Mäder K, Gohla S. Solid lipid nanoparticles (SLN) for controlled drug delivery—a review of the state of the art. *European journal of pharmaceuticals and biopharmaceutics*. 2000;50(1):161–177. Available from: [https://doi.org/10.1016/S0939-6411\(00\)00087-4](https://doi.org/10.1016/S0939-6411(00)00087-4).
6. Mohammadi-Samani S, Ghasemiyeh P. Solid lipid nanoparticles and nanostructured lipid carriers as novel drug delivery systems: applications, advantages and disadvantages. *Medknow*. 2018. Available from: <https://dx.doi.org/10.4103/1735-5362.235156>. doi:10.4103/1735-5362.235156.
7. Bhalekar MR, Pokharkar V, Madgulkar A, Patil N, Patil N. Preparation and Evaluation of Miconazole Nitrate-Loaded Solid Lipid Nanoparticles for Topical Delivery. *AAPS PharmSciTech*. 2009;10(1):289–296. Available from: <https://dx.doi.org/10.1208/s12249-009-9199-0>.
8. Kalam MA, Sultana Y, Ali A, Aqil M, Mishra AK, Chuttani K. Preparation, characterization, and evaluation of gatifloxacin loaded solid lipid nanoparticles as colloidal ocular drug delivery system. *Journal of Drug Targeting*. 2010;18(3):191–204. Available from: <https://dx.doi.org/10.3109/10611860903338462>.
9. Havens JP, Podany AT, Scarsi KK, Fletcher CV. Clinical Pharmacokinetics and Pharmacodynamics of Etravirine: An Updated Review. *Clinical Pharmacokinetics*. 2020;59(2):137–154. Available from: <https://dx.doi.org/10.1007/s40262-019-00830-9>.
10. Schiller DS, Youssef-Bessler M. Etravirine: A second-generation nonnucleoside reverse transcriptase inhibitor (NNRTI) active against NNRTI-resistant strains of HIV. *Clinical Therapeutics*. 2009;31(4):692–704. Available from: <https://dx.doi.org/10.1016/j.clinthera.2009.04.020>.
11. Ojewole E, Mackraj I, Naidoo P, Govender T. Exploring the use of novel drug delivery systems for antiretroviral drugs. *European Journal of Pharmaceutical and Biopharmaceutics*. 2008;70(3):697–710. Available from: <https://dx.doi.org/10.1016/j.ejpb.2008.06.020>.
12. Gupta S, Kesarla R, Chotai N, Misra A, Omri A. Systematic Approach for the Formulation and Optimization of Solid Lipid Nanoparticles of Efavirenz by High Pressure Homogenization Using Design of Experiments for Brain Targeting and Enhanced Bioavailability. *BioMed Research International*. 2017;2017:1–18. Available from: <https://dx.doi.org/10.1155/2017/5984014>.
13. Dwivedi P, Khatik R, Khandelwal K, Shukla R, Paliwal SK, Dwivedi AK, et al. Preparation and Characterization of Solid Lipid Nanoparticles of Antimalarial Drug Arteether for Oral Administration. *Journal of Biomaterials and Tissue Engineering*. 2014;4(2):133–137. Available from: <https://dx.doi.org/10.1166/jbt.2014.1148>.
14. Senthilkumar P, Arivuchelvan A, Jagadeeswaran A, Subramanian N, Senthilkumar C, Mekala P. Formulation, optimization and evaluation of enrofloxacin solid lipid nanoparticles for sustained oral delivery. *Asian Journal of Pharmaceutical and Clinical Research*. 2015;p. 231–236. Available from: [https://www.researchgate.net/publication/281738011\\_Formulation\\_optimization\\_and\\_evaluation\\_of\\_enrofloxacin\\_solid\\_lipid\\_nanoparticles\\_for\\_sustained\\_oral\\_delivery](https://www.researchgate.net/publication/281738011_Formulation_optimization_and_evaluation_of_enrofloxacin_solid_lipid_nanoparticles_for_sustained_oral_delivery).
15. Reddiah CV, Devi PR, Mukkanti K, Katari S. Estimation of Etravirine by UV-Visible Spectrophotometric Method in Tablet Dosage Forms and Its in Vitro Dissolution Assessment. *International Journal of Pharmaceutical Research and Development*. 2012;3(3):287–295.
16. Saha N. Comparison of the % drug release of drug and polymers (PVP K30 and PEG 6000) by using various buffers. *Indo Am. J Pharm Res*. 2014;4(1):815–834.
17. Parhi R, Suresh P. Production of solid lipid nanoparticles-drug loading and release mechanism. *J Chem Pharm Res*. 2010;2(1):211–218. Available from: <https://www.jocpr.com/articles/production-of-solid-lipid-nanoparticlesdrug-loading-and-release-mechanism.pdf>.
18. Nimbalkar UA, Dhoka MV, Sonawane PA. Formulation and optimization of cefpodoxime proxetil loaded solid lipid nanoparticles by box-behnken design. *Int J Res Ayur Pharm*. 2011;2(6):1779–1785. Available from: [https://ijrap.net/admin/php/uploads/714\\_pdf.pdf](https://ijrap.net/admin/php/uploads/714_pdf.pdf).
19. Dwivedi P, Khatik R, Khandelwal K, Shukla R, Paliwal SK, Dwivedi AK, et al. Preparation and Characterization of Solid Lipid Nanoparticles of Antimalarial Drug Arteether for Oral Administration. *Journal of Biomaterials and Tissue Engineering*. 2014;4(2):133–137. Available from: <https://dx.doi.org/10.1166/jbt.2014.1148>.
20. Liu W, Hu M, Liu W, Xue C, Xu H, Yang X. Investigation of the carbopol gel of solid lipid nanoparticles for the transdermal iontophoretic delivery of triamcinolone acetate. *International Journal of Pharmaceutics*. 2008;364(1):135–141. Available from: <https://dx.doi.org/10.1016/j.jipharm.2008.08.013>.
21. Freitas C, Müller RH. Effect of light and temperature on zeta potential and physical stability in solid lipid nanoparticle (SLN<sup>TM</sup>) dispersions. *International Journal of Pharmaceutics*. 1998;168(2):221–229. Available from: [https://dx.doi.org/10.1016/s0378-5173\(98\)00092-1](https://dx.doi.org/10.1016/s0378-5173(98)00092-1).
22. Ramesh K, Shekar BC, Khadgpathi P, Bhikshapathi DV, Gourav N. Enhancement of solubility and bioavailability of etravirine solid dispersions by solvent evaporation technique with novel carriers. *IOSR J Pharm Biol Sci*. 2015;10(4):30–41. Available from: <https://www.pharmaexcipients.com/wp-content/uploads/attachments/F010443041.pdf?t=1494431187>.
23. Castelli F, Puglia C, Sarpietro MG, Rizza L, Bonina F. Characterization of indomethacin-loaded lipid nanoparticles by differential scanning calorimetry. *International Journal of Pharmaceutics*. 2005;304(1–2):231–238. Available from: <https://dx.doi.org/10.1016/j.jipharm.2005.08.011>.
24. H RK, A JS, N DS. Solid Lipid Nanoparticle: A Review. *IOSR Journal of Pharmacy (IOSRPHR)*. 2012;2(6):34–44. Available from: <https://dx.doi.org/10.9790/3013-26103444>.
25. Pani NR, Nath LK, Acharya S, Bhuniya B. Application of DSC, IST, and FTIR study in the compatibility testing of nateglinide with different pharmaceutical excipients. *Journal of Thermal Analysis and Calorimetry*. 2012;108(1):219–226. Available from: <https://dx.doi.org/10.1007/s10973-011-1299-x>.
26. Fisher SR. JMP 8 Design of Experiments Guide. 1965. Available from: <https://citeseerx.ist.psu.edu/document?repid=rep1&type=pdf&doi=4c85db8e5dff392efea9930365d49a0ecf79abe3>.
27. Pawar YB, Purohit H, Valicherla GR, Munjal B, Lale SV, Patel SB, et al. Novel lipid based oral formulation of curcumin: Development and optimization by design of experiments approach. *International Journal of Pharmaceutics*. 2012;436(1–2):617–623. Available from: <https://dx.doi.org/10.1016/j.jipharm.2012.07.031>.
28. Blasi P, Giovagnoli S, Schoubben A, Puglia C, Bonina F, Rossi C, et al. Lipid nanoparticles for brain targeting I. Formulation optimization. *International Journal of Pharmaceutics*. 2011;419(1–2):287–295. Available from: <https://dx.doi.org/10.1016/j.jipharm.2011.07.035>.
29. Pouton CW, Porter CJH. Formulation of lipid-based delivery systems for oral administration: Materials, methods and strategies. *Advanced Drug Delivery Reviews*. 2008;60(6):625–637. Available from: <https://dx.doi.org/10.1016/j.addr.2007.10.010>.

30. Kovacevic A, Savic S, Vuleta G, Müller RH, Keck CM. Polyhydroxy surfactants for the formulation of lipid nanoparticles (SLN and NLC): Effects on size, physical stability and particle matrix structure. *International Journal of Pharmaceutics*. 2011;406(1-2):163–172. Available from: <https://dx.doi.org/10.1016/j.ijpharm.2010.12.036>.
31. Carbone C, Tomasello B, Ruozzi B, Renis M, Puglisi G. Preparation and optimization of PIT solid lipid nanoparticles via statistical factorial design. *European Journal of Medicinal Chemistry*. 2012;49:110–117. Available from: <https://dx.doi.org/10.1016/j.ejmech.2012.01.001>.
32. Pathak R, Dash RP, Misra M, Nivsarkar M. Role of mucoadhesive polymers in enhancing delivery of nimodipine microemulsion to brain via intranasal route. *Acta Pharmaceutica Sinica B*. 2014;4(2):151–160. Available from: <https://dx.doi.org/10.1016/j.apsb.2014.02.002>.
33. Chiappetta DA, Hocht C, Taira C, Sosnik A. Oral pharmacokinetics of the anti-HIV efavirenz encapsulated within polymeric micelles. *Biomaterials*. 2011;32(9):2379–2387. Available from: <https://dx.doi.org/10.1016/j.biomaterials.2010.11.082>.